

Very Strong Binding for a Neutral Calix[4]pyrrole Receptor Displaying Positive Allosteric Binding

Troels Duedal,[†] Kent A. Nielsen,[†] Gunnar Olsen,[†] Charlotte B. G. Rasmussen,[†] Jacob Kongsted,[†] Eric Levillain,[‡] Tony Breton,[‡] Eigo Miyazaki,[§] Kazuo Takimiya,^{||} Steffen Bähring,^{*,†} and Jan O. Jeppesen^{*,†}

[†]Department of Physics, Chemistry, and Pharmacy, University of Southern Denmark, Campusvej 55, Odense M DK-5230, Denmark

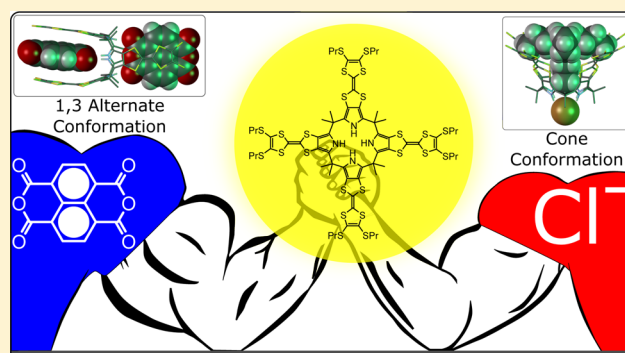
[‡]MOLTECH Anjou - UMR 6200 du CNRS, Université d'Angers, 2 Bd Lavoisier, Angers F-49045 Cedex, France

[§]Department of Applied Chemistry, Graduate School of Engineering, Hiroshima University, Higashi-Hiroshima 739-8527, Japan

^{||}Emergent Molecular Function Research Group, RIKEN Center for Emergent Matter Science (CEMS), 2-1 Hirosawa, Wako, Saitama 351-0198, Japan

Supporting Information

ABSTRACT: The dual-analyte responsive behavior of tetraTTF-calix[4]pyrrole receptor **1** has been shown to complex electron-deficient planar guests in a 2:1 fashion by adopting a so-called 1,3-alternate conformation. However, stronger 1:1 complexes have been demonstrated with tetraalkylammonium halide salts that defer receptor **1** to its cone conformation. Herein, we report the complexation of an electron-deficient planar guest, 1,4,5,8-naphthalenetetracarboxylic dianhydride (NTCDA, **2**) that champions the complexation with **1**, resulting in a high association constant $K_a = 3 \times 10^{10} \text{ M}^{-2}$. The tetrathiafulvalene (TTF) subunits in the tetraTTF-calix[4]-pyrrole receptor **1** present a near perfect shape and electronic complementarity to the NTCDA guest, which was confirmed by X-ray crystal structure analysis, DFT calculations, and electron density surface mapping. Moreover, the complexation of these species results in the formation of a charge transfer complex (2_2C1) as visualized by a readily apparent color change from yellow to brown.



INTRODUCTION

Considerable efforts have been focused on the preparation of supramolecular host systems with the capability of recognizing specific chemical species through weak noncovalent interactions.^{1–3} In this context, the use of 1,4,5,8-naphthalene diimides⁴ (NDIs) appears particularly attractive, on account of their intriguing properties as electron-deficient and aromatic species, their ability to form face-to-face aromatic interactions with electron donors, and their ease of functionalization. Since the late 20th century, many systems containing NDIs have been studied in the context of semiconducting materials,⁵ sensors,^{6,7} foldamers,^{8,9} catenanes,¹⁰ and rotaxanes.^{11,12} Even though NDI has received considerable attention, much less time has been devoted to its precursor molecule, the commercially available 1,4,5,8-naphthalenetetracarboxylic dianhydride (NTCDA, **2**), and only a few examples of receptors exist.¹³ To the best of our knowledge, no pure organic receptors occur for NTCDA.

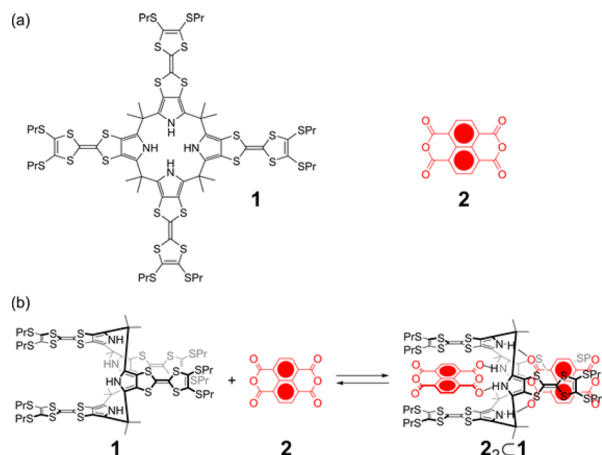
Herein, we report a remarkably strong complexation between the neutral tetrathiafulvalene (TTF)-substituted calix[4]-pyrrole^{14–18} receptor **1** and the guest NTCDA **2** (Scheme 1). Calix[4]pyrrole has been shown to act as receptor for neutral substrates,^{19–21} in its 1,3-alternate conformation, and in

particular the TTF-substituted calix[4]pyrroles^{14–18} have been shown to complex electron-deficient aromatic guests such as 1,3,5-trinitrobenzene (TNB) and 2,4,6-trinitrotoluene (TNT). The recognition behavior of calix[4]pyrroles toward anions,^{15,17,22} in its cone conformation, is also widely appreciated, and binding constants as high as $K_a = 1.5 \times 10^7 \text{ M}^{-1}$ have been reported¹⁷ for chloride anions (as its tetraethylammonium (TEA) salt). On account of the mutual complementarity between the electron-donating TTF subunits of receptor **1** and the electron-accepting NTCDA guests, complexation was expected to take place upon mixing **1** and **2**. However, it was unexpected that the complex formed (2_2C1) exhibited an overall complexation strength that is among the highest reported for neutral complexes^{23,24} and comparable to charged systems such as cucurbituril-guests-binding^{25,26} and bisporphyrin macrocycles²⁷ for C_{60} . This makes receptor **1** attractive, not only for NTCDA sensing, but also for the preparation of supramolecular systems containing NDI and its analogues pyromellitic diimides and perylene diimides.

Received: December 8, 2016

Published: January 25, 2017

Scheme 1. (a) Chemical Structures of Receptor **1** and Guest **2**, and (b) Mechanistic Scheme Displaying the Proposed Complexation between **1** and **2** and the Complex 2_2C1



RESULTS AND DISCUSSION

Crystal Structure. Initial evidence for the complexation between **1** and **2** came from single-crystal X-ray diffraction analysis. Diffraction grade crystals were grown by slow diffusion of an *n*-hexane layer into a CH_2Cl_2 solution containing **1** (1 mM) and **2** (2 mM). The resulting structural analysis (Figure 1) revealed a solid-state structure containing one tetraTTF-

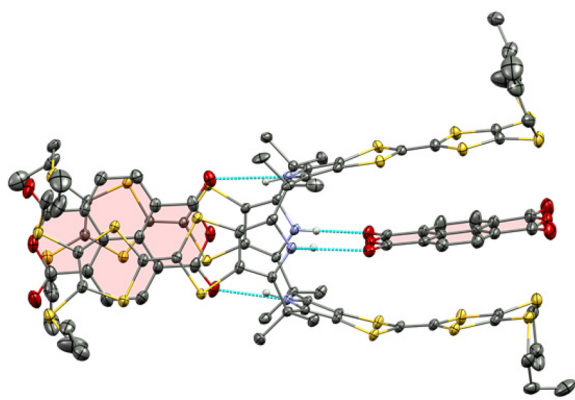


Figure 1. Single-crystal X-ray structure of the complex 2_2C1 illustrating the four hydrogen-bond interactions taking place between the NH protons of **1** and the carbonyl oxygen atoms of **2**. Ellipsoids are scaled at the 30% probability level. Nonparticipating hydrogen atoms have been removed for clarity.

calix[4]pyrrole receptor **1** complexed with two guest molecules **2**, forming a charge transfer (CT) complex. The two guest molecules are oriented parallel relative to the TTF “arms” having one set of the anhydride oxygens pointing toward the NH protons and involved in hydrogen bonding in the solid state. The interplanar distance between two TTF units is in the range of 6.9–7.0 Å, which is close to the optimal distance of 7 Å for CT interactions.²⁸

1H NMR Spectroscopic Investigations. Support for the interaction between **1** and **2** in solution was evident when comparing the 1H NMR spectrum ($CDCl_3$, 500 MHz, 298 K) of **1** with that of a 1:2 mixture of **1** and **2** (Figure 2c). The 1H NMR spectrum of **1** reveals a signal resonating at $\delta = 7.15$ ppm, which can be assigned to the free NH protons. Upon addition of 2 equiv of **2** to this solution, the signals corresponding to the

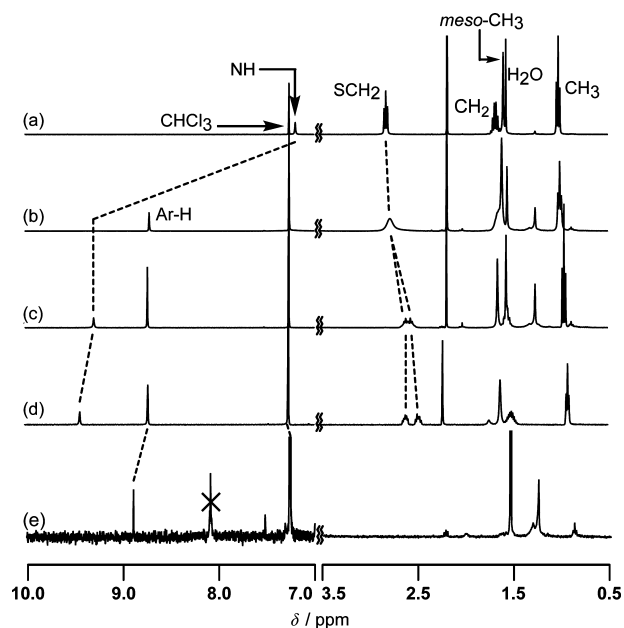


Figure 2. Partial 1H NMR spectra ($CDCl_3$, 500 MHz, 298 K): (a) **1** (2 mM), (b) **1** + 1 equiv of **2**, (c) **1** + 2 equiv of **2**, (d) the solution from (c) at 228 K, and (e) **2** (saturated).

resonances of the NH protons are shifted downfield to $\delta = 9.28$ ppm ($\Delta\delta = +2.13$ ppm). The large downfield shift can be attributed to the combination of CT interaction and hydrogen bonding taking place between **1** and **2**. The aromatic CH protons of **2** are sandwiched between two shielding TTF subunits and can be found as a sharp signal resonating at $\delta = 8.72$ ppm ($\Delta\delta = -0.18$ ppm) as compared to pure **2** (Figure 2e). In the aliphatic region of the spectrum, the signals from the protons in the thiopropyl chains are found to be upfield shifted ($\Delta\delta = -0.06$, -0.12 , and $-0.21/-0.25$ ppm). In particular, the SCH_2 protons are observed as two broad signals at 298 K, which upon cooling to 228 K sharpens into two multiplets (dt, $J = 13.1$ and 6.7 Hz). This finding can, most likely, be ascribed to the fact that the strong complexation between **1** and **2** leads to a conformationally restricted complex where the two SCH_2 protons of the thiopropyl chains become chemically different resulting in an AB type system at low temperature.²⁹ 1H NMR titration of **2** into a solution of **1** (see Figure S1) resulted in an immediate broadening of the NH proton resonances of **1** ($\delta = 7.16$ ppm). Upon further addition of **2** (0.8 equiv), the resonance at $\delta = 7.16$ ppm disappeared, whereas a new signal resonating at $\delta = 9.28$ ppm is observed, which can be assigned to the complexed NH protons in the 2_2C1 complex.

Optical and Electrochemical Investigations. Formation of the complex between **1** and **2** was also studied using absorption spectroscopy. The addition of 2 equiv of **2** to a solution of **1** gives rise to a color change from yellow to brown and the appearance of a CT absorption band centered at 990 nm in the absorption spectrum (Figure 3). An absorption spectroscopic titration experiment was carried out in CH_2Cl_2 solution (5.6 μM of **1**) to determine the association constants (K_1 , K_2 , and K_3) for the interaction between receptor **1** and guest **2**. The guest binding event was visualized by following the progressive color change produced as **2** was added to receptor **1** (Figure 3, inset). Plots of the associated changes in absorption intensity as a function of guest concentration were

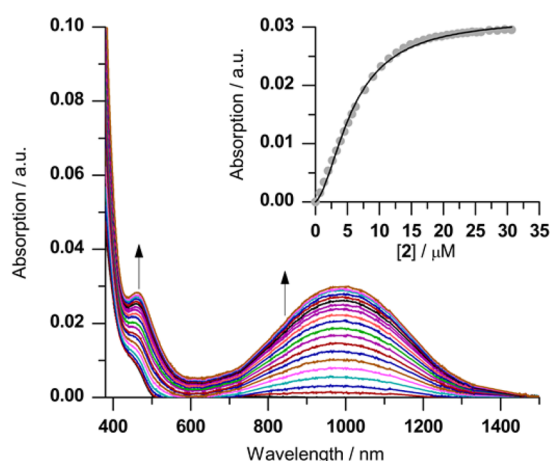


Figure 3. Absorption spectroscopic titration of receptors **1** ($5.6 \mu\text{M}$) with **2** (CH_2Cl_2 , 295 K). Increasing amounts of **2** were added for each absorption spectra (0–6 equiv) leading to a broad CT band centered at $\lambda = 990 \text{ nm}$. Inset shows the calculated binding isotherm derived by using the two-site Adair equation³⁰ for the absorption at $\lambda = 1000 \text{ nm}$.

then used to construct the binding isotherm (Figure 3, inset). The data were fitted to a two-site Adair equation³⁰ ($R^2 > 0.998$), and the two microscopic binding constants could be determined to $K_1 = 2.9 \times 10^4 \text{ M}^{-1}$ and $K_2 = 1.0 \times 10^6 \text{ M}^{-1}$, respectively ($K_a = 2.9 \times 10^{10} \text{ M}^{-2}$). Fitting the data to a Hill equation³¹ ($R^2 > 0.993$) gave an association constant of $K_a = 1.7 \times 10^9 \text{ M}^{-2}$ and a Hill coefficient of $n = 1.57$ (see Figure S8), showing a strong cooperative binding effect at the second binding site. To the best of our knowledge, this is the highest reported association constant for a TTF-calixpyrrole macrocyclic host and any neutral or charged species.

The strong complexation and cooperative binding effect can be explained by the ideal geometry of guest **2** for the binding sites of **1** and the inductive effect that the first binding exerts on the second binding site of receptor **1** (Figure 4).

To verify the strong complexation of the neutral complex, another complementary spectroscopic method was used. Utilizing the fluorescent output of **2**, a titration of **2** ($5.6 \mu\text{M}$) with **1** was carried out in CHCl_3 (Figure 5). The broad fluorescence at 360–450 nm is efficiently quenched by 95% upon addition of 1 equiv of **1** and >99% quenched at 2 equiv of **2**. The data could be fitted to a 2:1 binding isotherm³² ($R^2 > 0.999$), giving K_1 and K_2 as 6.0×10^4 and $5.0 \times 10^5 \text{ M}^{-1}$, respectively ($K_a = 3.0 \times 10^{10} \text{ M}^{-2}$).

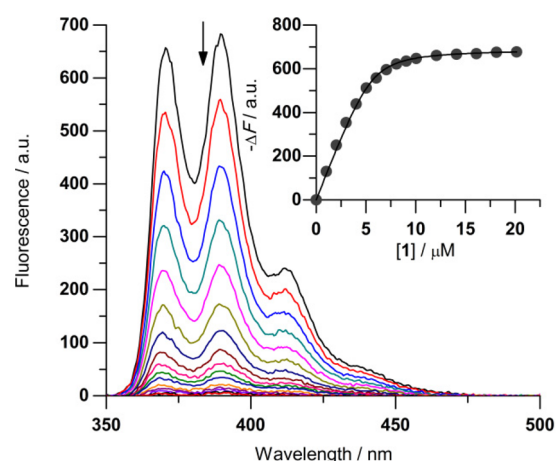


Figure 5. Fluorescence emission spectra of **2** ($5.6 \mu\text{M}$, $\lambda_{\text{ex}} = 330 \text{ nm}$) upon addition of increasing amounts of **1** (CHCl_3 at 295 K). Inset show the change in fluorescence at $\lambda = 390 \text{ nm}$ with increasing concentration of **1** fitted to a 2:1 binding isotherm.³²

This success led us to consider the redox processes of the TTF subunits of **1** and the NTCDA guest **2** as a possible transducer of the recognition event. Cyclic voltammetry (CV) was used to probe the putative NTCDA-induced changes in the redox potentials. The deconvoluted voltammogram (Figure 6)

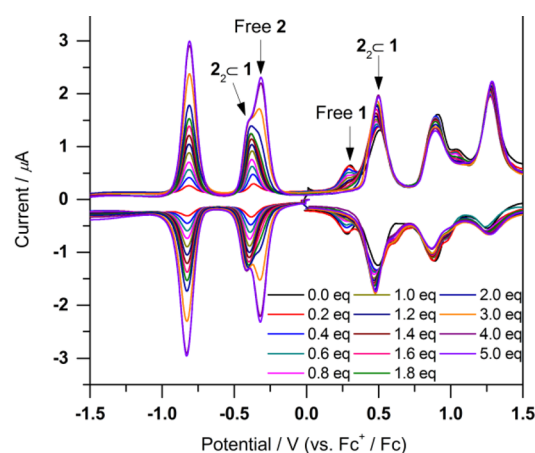


Figure 6. Deconvoluted cyclic voltammograms of receptor **1** (0.01 mM in CH_2Cl_2) recorded at 100 mV s^{-1} after the addition of successive aliquots of **2** (reference electrode, Fc^+/Fc ; supporting electrolyte, tetrabutylammonium hexafluorophosphate (TBAPF_6 , 0.1 M)).

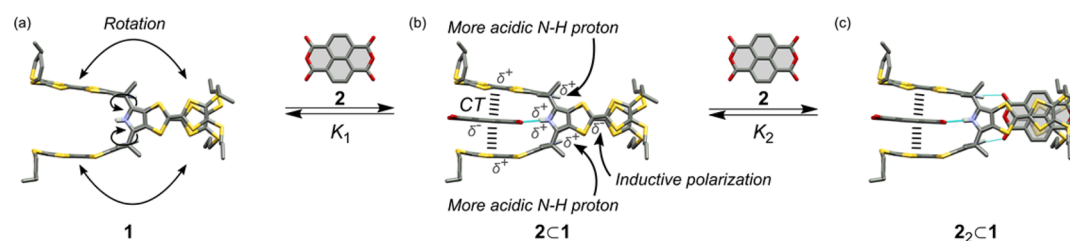


Figure 4. Illustration of the cooperative binding modes of receptor **1** upon binding two guests **2**. (a) The free receptor predominantly obtains the 1,3-alternate conformation with a high degree of flexibility in the two binding sites. (b) When one molecule of **2** is bound, the receptor **1** obtains a more rigid 1,3-alternate conformation due to the CT interactions between the TTFs and **2** and the hydrogen-bonding interactions between the pyrrole NH protons of **1** and the oxygen atoms of **2**. These interactions lead to a hyperpolarization of **1** where the TTFs of the vacant binding site become more electron-rich and the vacant pyrrole NH protons become more acidic. (c) The improved binding of the second binding site results in a stronger complexation and an overall stabilized $2_2<1$ complex.

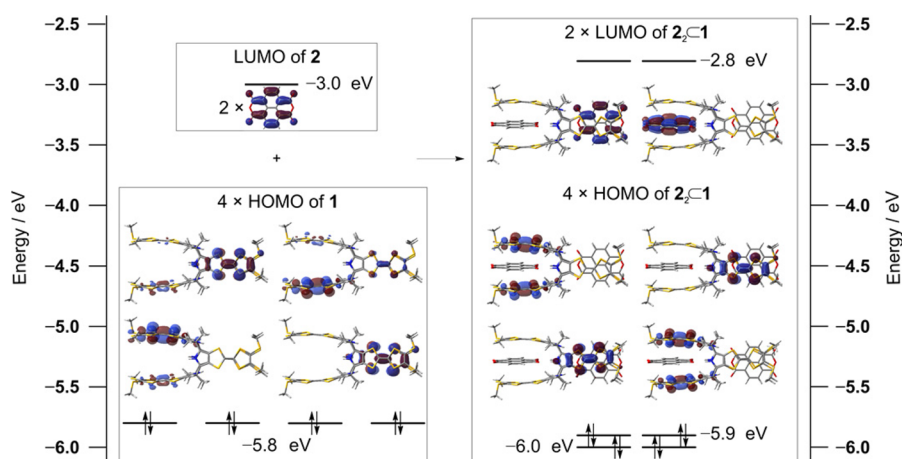


Figure 7. Energy level diagram (eV) of **1**, **2**, and 2_2C1 (M05-2X/6-31+G**) using the PCM model of $CHCl_3$.³³

shows that progressive addition of **2** to a solution of receptor **1** results in the disappearance of the first oxidation process ($E_{1/2}^1 = 0.297$ V) for the TTF units in **1**, corresponding to the gradual loss of uncomplexed **1** and an appearance of two new redox processes at ($E_{1/2}^1 = -0.371$ V and $E_{1/2}^2 = -0.813$ V) corresponding to first reduction of complexed **2** and subsequent second reduction of uncomplexed **2**. Addition of more than 2 equiv of **2** resulted in the appearance of a new redox process ($E_{1/2}^1 = -0.314$ V), matching uncomplexed **2**. These results supports that a strong complexation between receptor and guest is taking place in solution.

DFT Calculations. The structure and properties (geometry, CT interaction, and excitation) of **1**, **2**, and the 2_2C1 complex were also investigated through density functional theory (DFT) calculation in $CHCl_3$ modeled by the polarizable continuum model (PCM).³³ Full geometry optimizations were performed at the M05-2X/6-31G* level of theory (Figure 7). For the uncomplexed receptor, the four HOMOs (highest-occupied molecular orbital) are predominantly localized on the four individual TTF units. The two LUMOs (lowest-unoccupied molecular orbitals) of the free guest show orbitals with a nodal plane running through the middle. Upon complexation, the energies of the four HOMOs are paired and show shifts to lower energies (-5.9 and -6.0 eV) as a result of stabilization, together with a concurrent increase of the LUMOs of **2** (-2.8 eV). These rearrangements are consistent with a CT interaction among the frontier MOs. In the complex pairs of HOMOs are mixed together, indicating that the CT interaction between **1** and encapsulated **2** acts as an electronic bridge. The DFT calculations confirmed that **2** is a close to perfect fit for **1**, with pairs of TTF “arms” closely wrapped around the two guest units. Beside the very high binding constants, one of the most significant features of the 2_2C1 complex is the combination of shape and electronic complementarity between the TTF units present in **1** and the guest **2**. This complementarity is evident from the charge density plot (Figure 8), which shows that free receptor **1** has a partial positive charge on the NH protons and partial negative charge on the sulfur atoms. For **2**, partial negative and positive charges are found on the oxygen atoms and the carbonyl carbons, respectively, giving rise to overlap between oppositely partial charged surfaces. In the complex, the charge distribution is less pronounced as a result of CT-interaction. Natural bond orbital (NBO) analysis shows a CT interaction in the opposite direction of the hydrogen bond where 0.17 electrons is transferred from **1** to **2**, indicating a

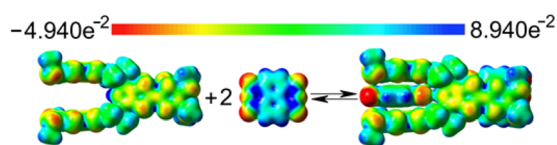


Figure 8. Electron density surfaces (isovalue = 0.008) mapped according to the value of the electrostatic potential of respective receptor **1** and guest **2** as well as their complex 2_2C1 .

significant CT stabilization. Single-point time-dependent DFT calculations (CAM-B3LYP/6-31+G**) were carried out to investigate the CT excitation in the 2_2C1 complex; the lowest excitation is found to be a result of excitation from HOMO and HOMO-1 to LUMO and LUMO+1 (1.61 eV/770 nm) consistent with a CT-band. The excitation energy is found to be overestimated by about 30% as was also seen in the literature.³⁴

Competition Analysis. The variety of which receptor **1** can complex different guests such as anions, neutral, and charged planar guests has been an intriguing quality of the TTF-calix[4]pyrrole system. Most prominently, it binds anions in the so-called cone conformation, wherein it becomes a good host for spherical guests such as fullerenes C_{60} and C_{70} . It is in the cone conformation that the highest association constant ($K_a = 1.5 \times 10^7$ M⁻¹ for TEACl)¹⁷ has been reported. To probe the competitive binding of **1**, we prepared a solution of **1** (1.1 mM) and 2 equiv of **2** (2.2 mM) in $CDCl_3$ (Figure 9). Monitoring the pyrrole NH resonances located at $\delta = 9.28$ ppm (Figure 9a) for the complex 2_2C1 , aliquots of tetrabutylammonium chloride (TBACl, $K_a = 2.5 \times 10^6$ M⁻¹)¹⁵ were subsequently added. Addition of 10 equiv of TBACl (Figure 9b) to the complex solution resulted in a slight broadening and decrease of the NH proton resonances at $\delta = 9.28$ ppm, while a broad singlet arises at $\delta = 10.82$ ppm that can be assigned to **1** in its chloride-bound cone conformation ($1 \cdot Cl^-$). Integration of the two signals corresponding to the complexes of $1 \cdot Cl^-$ and 2_2C1 gave a ratio of 1:6.3, respectively. This finding clearly indicates that the complex 2_2C1 is the most stable complex. Further additions of TBACl to the solution containing the complex 2_2C1 resulted in further shifts in the complex ratio of 1:1.1 (Figure 9c, 30 equiv of TBACl) and 1:0.3 (Figure 9d, 50 equiv of TBACl) for the complexes of $1 \cdot Cl^-$ and 2_2C1 , respectively. It is appreciated that the competition experiment for receptor **1** requires a change of conformation from the more stable 1,3-alternate conformation to the cone conformation, which may offer further stabilization

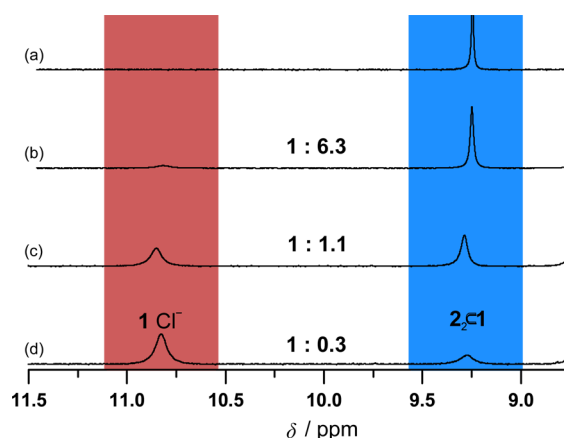


Figure 9. Partial ^1H NMR spectra (CDCl_3 , 400 MHz, 298 K) of (a) **1** (1.1 mM) + 2 equiv of **2**, (b) **1** + 2 equiv of **2** + 10 equiv of TBACl, (c) **1** + 2 equiv of **2** + 30 equiv of TBACl, and (d) **1** + 2 equiv of **2** + 50 equiv of TBACl.

of the already formed 1,3-alternate complex of 2_2C1 . However, this analysis supports the notion that the binding strength of receptor **1** for **2** should be of the same order as that for TBACl or higher.

CONCLUSION

In summary, the tetraTTF-calix[4]pyrrole receptor **1** features the combination of hydrogen bonding and charge transfer interaction, resulting in a very effective association of the 1,4,5,8-naphthalenetetracarboxylic dianhydride guest (**2**). Solution and solid-phase characterization was employed to describe the complexation event. DFT calculations and electron density surface mapping confirmed the exquisite combinations of shape and electronic complementarity that exist between the TTF units present in **1** and the guest NTCDA. The stabilized 1,3-alternate complex 2_2C1 is shown to be favored over chloride anion binding (TBA^+ salt in the cone conformation). We are currently exploring the stability of the complexes formed between the receptor **1** and NDIs, pyromellitic dianhydride, pyromellitic diimides, and their analogues, and preliminary results also indicate strong complexation with these guests.

EXPERIMENTAL SECTION

TetraTTF-calix[4]pyrrole¹⁴ **1** was synthesized according to known literature procedures. NTCDA was purchased from Sigma-Aldrich and used as received. ^1H NMR spectra were recorded on a 400 MHz NMR spectrometer at 298 K. The variable-temperature and 2D ^1H NMR spectra were recorded on a 500 MHz NMR spectrometer. The NMR samples were dissolved in CDCl_3 and TMS, or the residual solvent was used as internal standard. Solvent signals were assigned according to Nudelman et al.³⁵ Absorption and emission spectroscopic studies were carried out using spectroscopic grade solvents. Cyclic voltammetry (CV) was performed in a three-electrode cell equipped with a platinum millielectrode, a platinum wire counter-electrode, and a silver wire used as quasi-reference electrode. The electrochemical experiments were carried out under dry and oxygen-free atmosphere ($\text{H}_2\text{O} < 1$ ppm, $\text{O}_2 < 1$ ppm) in CH_2Cl_2 [**1**] = 10 μM) with Bu_4NPF_6 (TBAPF_6) (0.1 M) as supporting electrolyte. The voltammograms were recorded with positive feedback compensation. On the basis of repetitive measurements, the absolute errors of potentials were estimated to be around ± 5 mV. Crystallographic data were collected on a diffractometer with Mo $K\alpha$ radiation ($\lambda = 0.71073$ Å).

ASSOCIATED CONTENT

Supporting Information

The Supporting Information is available free of charge on the ACS Publications website at DOI: 10.1021/acs.joc.6b02944.

X-ray crystallographic data for compound **1** (CIF)

^1H NMR titration and variable-temperature spectra, UV-vis and fluorescence titration spectra with calculated binding isotherms, CV data, DFT calculations with orbital energies, and crystallographic data (PDF)

AUTHOR INFORMATION

Corresponding Authors

*E-mail: sbahring@sdu.dk.

*E-mail: joj@sdu.dk.

ORCID

Gunnar Olsen: 0000-0003-2254-3543

Kazuo Takimiya: 0000-0002-6001-1129

Steffen Bähring: 0000-0001-5113-2458

Jan O. Jeppesen: 0000-0002-3088-2994

Notes

The authors declare no competing financial interest.

ACKNOWLEDGMENTS

This work is dedicated to Professor Jonathan L. Sessler on the occasion of his 60th birthday. This work was supported by the Danish Natural Science Research Council (FNU, project no. 272-08-0047), The Danish Council for Independent Research, Technology, and Production Sciences (FTP, project 5054-00052), the Lundbeck Foundation (project no. R49-A5379), the Carlsberg Foundation (project no. 2010-01-0789), and the University of Southern Denmark (SDU).

REFERENCES

- Rebek, J. *Acc. Chem. Res.* **1984**, *17*, 258–264.
- Takeuchi, M.; Ikeda, M.; Sugasaki, A.; Shinkai, S. *Acc. Chem. Res.* **2001**, *34*, 865–873.
- Atwood, J. L.; Steed, J. W. *Encyclopedia of Supramolecular Chemistry*; Marcel Dekker: New York, 2004; Vols. 1–2.
- Bhosale, S. V.; Jani, C. H.; Langford, S. J. *Chem. Soc. Rev.* **2008**, *37*, 331–342.
- Katz, H.; Lovinger, A.; Johnson, J.; Kloc, C.; Siegrist, T.; Li, W.; Lin, Y.; Dodabalapur, A. *Nature* **2000**, *404*, 478–481.
- Takenaka, S.; Yamashita, K.; Takagi, M.; Uto, Y.; Kondo, H. *Anal. Chem.* **2000**, *72*, 1334–1341.
- Mukhopadhyay, P.; Iwashita, Y.; Shirakawa, M.; Kawano, S.-I.; Fujita, N.; Shinkai, S. *Angew. Chem., Int. Ed.* **2006**, *45*, 1592–1595.
- Gabriel, G. J.; Sorey, S.; Iverson, B. L. *J. Am. Chem. Soc.* **2005**, *127*, 2637–2640.
- Reczek, J. J.; Iverson, B. L. *Macromolecules* **2006**, *39*, 5601–5603.
- Hansen, J.; Feeder, N.; Hamilton, D.; Gunter, M.; Becher, J.; Sanders, J. *Org. Lett.* **2000**, *2*, 449–452.
- Vicic, D. A.; Odom, D. T.; Nunez, M. E.; Gianolio, D. A.; McLaughlin, L. W.; Barton, J. K. *J. Am. Chem. Soc.* **2000**, *122*, 8603–8611.
- Iijima, T.; Vignon, S. A.; Tseng, H.-R.; Jarrosson, T.; Sanders, J. K. M.; Marchioni, F.; Venturi, M.; Apostoli, E.; Balzani, V.; Stoddart, J. F. *Chem. - Eur. J.* **2004**, *10*, 6375–6392.
- Kim, D.; Lee, S.; Gao, G.; Seok Kang, H.; Ko, J. *J. Organomet. Chem.* **2010**, *695*, 111–119.
- Nielsen, K. A.; Cho, W.-S.; Jeppesen, J. O.; Lynch, V. M.; Becher, J.; Sessler, J. L. *J. Am. Chem. Soc.* **2004**, *126*, 16296–16297.
- Nielsen, K. A.; Cho, W.-S.; Lyskawa, J.; Levillain, E.; Lynch, V. M.; Sessler, J. L.; Jeppesen, J. O. *J. Am. Chem. Soc.* **2006**, *128*, 2444–2451.

- (16) Park, J. S.; Le Derf, F.; Bejger, C. M.; Lynch, V. M.; Sessler, J. L.; Nielsen, K. A.; Johnsen, C.; Jeppesen, J. O. *Chem. - Eur. J.* **2010**, *16*, 848–854.
- (17) Park, J. S.; Karnas, E.; Ohkubo, K.; Chen, P.; Kadish, K. M.; Fukuzumi, S.; Bielawski, C. W.; Hudnall, T. W.; Lynch, V. M.; Sessler, J. L. *Science* **2010**, *329*, 1324–1327.
- (18) Davis, C. M.; Lim, J. M.; Larsen, K. R.; Kim, D. S.; Sung, Y. M.; Lyons, D. M.; Lynch, V. M.; Nielsen, K. A.; Jeppesen, J. O.; Kim, D.; Park, J. S.; Sessler, J. L. *J. Am. Chem. Soc.* **2014**, *136*, 10410–10417.
- (19) Shao, S.; Guo, Y.; He, L.; Jiang, S.; Yu, X. *Tetrahedron Lett.* **2003**, *44*, 2175–2178.
- (20) Allen, W. E.; Gale, P. A.; Brown, C. T.; Lynch, V. M.; Sessler, J. L. *J. Am. Chem. Soc.* **1996**, *118*, 12471–12472.
- (21) Furusho, Y.; Aida, T. *Chem. Commun.* **1997**, 2205–2206.
- (22) Gale, P. A.; Anzenbacher, P., Jr.; Sessler, J. L. *Coord. Chem. Rev.* **2001**, *222*, 57–102.
- (23) Huerta, E.; Isla, H.; Pérez, E. M.; Bo, C.; Martín, N.; de Mendoza, J. *J. Am. Chem. Soc.* **2010**, *132*, 5351–5353.
- (24) Zeng, H.; Miller, R. *J. Am. Chem. Soc.* **2000**, *122*, 2635–2644.
- (25) Kim, H.-J.; Heo, J.; Jeon, W. S.; Lee, E.; Kim, J.; Sakamoto, S.; Yamaguchi, K.; Kim, K. *Angew. Chem., Int. Ed.* **2001**, *40*, 1526–1529.
- (26) Moghaddam, S.; Yang, C.; Rekharsky, M.; Ko, Y. H.; Kim, K.; Inoue, Y.; Gilson, M. K. *J. Am. Chem. Soc.* **2011**, *133*, 3570–3581.
- (27) Tashiro, K.; Aida, T. *Chem. Soc. Rev.* **2007**, *36*, 189–197.
- (28) Hunter, C. A.; Sanders, J. K. M. *J. Am. Chem. Soc.* **1990**, *112*, 5525–5534.
- (29) Indirect support for the proposed orientation between receptor and guest came from NOESY NMR studies (CDCl₃, 233 K); where no cross-peaks corresponding to close noncovalent contacts between the Ar–H and NH protons were observed (see [Figure S4](#)), NOE signals are to be expected if the guest is oriented in a perpendicular fashion with respect to the host.
- (30) Adair, G. S. *J. Biol. Chem.* **1925**, *63*, 529–545.
- (31) Hill, A. V. *J. Physiol.* **1910**, *40*, 190–224.
- (32) Thordason, P. *Chem. Soc. Rev.* **2011**, *40* (3), 1305–1323.
- (33) In the DFT calculations, the eight thiopropyl chains have been substituted with thiomethyl groups to reduce the calculation time.
- (34) Albert, V. V.; Ivanov, S. A.; Tretiak, S.; Kilina, S. V. *J. Phys. Chem. C* **2011**, *115*, 15793–15800.
- (35) Gottlieb, H. E.; Kotlyar, V.; Nudelman, A. *J. Org. Chem.* **1997**, *62*, 7512–7515.